IMPACT OF COMPONENT PERFORMANCE ON THE ALLAM CYCLE EFFICIENCY: AN EXERGY ANALYSIS

Gnandjuet Gaston Brice Dago[1], Guido Francesco Frate[1], Andrea Baccioli[1], Lorenzo Ferrari[1]*, Emanuela Alfarano[2], Alessandro Colnago[2]

[1]University of Pisa, DESTEC, Pisa, Italy

[2]Baker Hughes, Florence, Italy

lorenzo.ferrari@unipi.it

ABSTRACT

Carbon capture technologies represent a crucial step towards the decarbonization of power production. The most common alternatives focus on separating the CO_2 from the power plant's exhaust, which markedly increases the power plant's footprint and complexity and reduces the net power output. A promising alternative is innovative power cycle development, which allows for a much easier CO_2 separation. The Allam cycle represents one of the most advanced and close to deployment of these cycles. The Allam cycle is a semi-closed cycle with oxyfuel combustion, which allows for the CO_2 direct separation from the cycle fluid in the supercritical state – a considerable advantage compared to post-combustion CO_2 removal technologies. Here, the focus is on a straightforward configuration with the following main parts: compression, internal heat regeneration, power production, heat rejection, water condensation, and separation, designed to produce up to 300 MW. The paper focuses on the Allam cycle performance analysis at different combustor outlet temperatures and recuperator dimensions, highlighting the actual cycle performance when conservative considerations are made compared to the assumptions and results already obtained in the literature. Results demonstrate that maximum recuperator UA from 30000 to 45000 kW/K is required, and a reduction of the combustor outlet temperatures from the highest to the lowest analysed values leads to a decrease in the net electric efficiency of around 5 percentage points. An exergy analysis is also conducted to examine the performance of each component and its impact on the overall system in terms of losses, helping to pinpoint the cycle's sources of thermodynamic inefficiencies at the component level.

1 INTRODUCTION

The global community needs to reduce greenhouse gas emissions, mainly CO_2, to combat climate change. Currently, efforts are focused on utilizing nuclear and renewable energy sources. However, the IPCC 5th assessment suggests that a broader range of low-carbon energy sources (IPCC Panel, 2014), including carbon capture and sequestration, is mandatory to meet climate targets. The absence of carbon capture and sequestration in energy scenarios leads to fewer instances of maintaining global temperature rise within agreed limits and higher costs. There are three main methods for capturing CO_2 from fossil fuel-based power generation: post-combustion, pre-combustion, and oxy-combustion (Figueroa et al., 2008; Wall, 2007).. In particular, Oxy-combustion technology burns fuel in an oxygen-rich environment, resulting in flue gas with a high CO_2 concentration, making removing it easier. While commercial pre- and post-combustion are already widely available, oxy-combustion technology is still developing despite already being realized on a small scale (Rubin et al., 2012). The Allam cycle presents a solution by utilizing hydrocarbon energy reserves cleanly and economically, capturing and either storing or reusing CO_2 produced from combustion. It was first introduced in Kyoto at GHGT-11(R. J. Allam et al., 2013). The recently proposed Allam cycle development has been undertaken by NET Power (R. Allam et al., 2017). It is a semi-closed cycle that requires a cryogenic air separation unit (ASU) for oxygen production, a high energy consumption system that reduces the cycle performance. Nevertheless, the cycle takes advantage of the thermodynamic properties of CO_2, minimizing energy

https://doi.org/10.52202/077185-0144

losses compared to steam-based cycles, reaching high efficiencies and low capital costs, and does not need additional equipment or processes to capture, purify and compress CO_2 (Chowdhury et al., 2016). According to the report published by the International Energy Agency (IEA) Green House Gas Program (Mancuso, 2015), the NET power cycle is considered the most promising semi-closed oxy-combustion option in terms of efficiency, with a net electric efficiency of around 55% compared to the SCOC-CC (Bolland & Mathieu, 1998), S-GRAZ (Jericha et al., 2008) and MATIANT (Iantovski & Mathieu, 1997) configurations that achieve respectively efficiencies about 49.3%, 49.2% and 52%. Many works on the Allam cycle in the literature demonstrate its promising thermodynamic and economic performance thanks to ideal considerations for modelling its key components. However, in-depth analyses of the behaviour of the recuperator are lacking. This study aims to show, starting from a base case referring to what has been studied in the literature, how the whole system behaves for different working conditions of the recuperator as well as to highlight how the causes of inefficiency are distributed among the various components for different operating conditions through an exergy analysis.

2 MATERIALS AND METHODS

The paper illustrates the Allam cycle performance at various operating conditions with different combustor outlet temperatures (COT) and recuperator pinch-points to assess their impact on the cycle's efficiency. Thus, based on the assumptions made to the recuperator, the cycle efficiency is calculated as a function of the pinch-point, also exploring hot-side temperature differences lower than the reference value. Plant inefficiency sources are investigated through an exergy analysis.

2.1 Cycle Process Description

A simplified process flow diagram of the Allam cycle is presented in Figure 1, highlighting its main features. Pressurized natural gas, oxygen from ASU and high-pressure recycled carbon dioxide react in the combustor to produce a high-temperature gas. The gas is directed to the turbine, where expansion occurs with a pressure ratio of around 10. The exhaust gas from the turboexpander is cooled through the recuperator, reheating the recycled CO_2 before entering the combustor. Water is subsequently separated by condensation, and the CO_2 stream is submitted to compression processes and reheated in the recuperator. Furthermore, the excess heat from ASU is recovered to improve the recuperator performance. Finally, a small quantity of CO_2 is exported from the system to control the CO_2 flow at the combustor inlet.

2.2 Simulation Model Description

Flowsheets description of the base case

In Figure 1, a synthesized flow diagram of the Allam cycle is presented. The natural gas, considered pure methane, is brought to a pressure above 300 bar (Mancuso, 2015) by the C-1 multistage and inter-refrigerated compression train before being placed in the combustion chamber. Combustion occurs under stoichiometric conditions in the presence of the oxidant (blue stream), containing oxygen above 99% of purity produced by ASU and most of the recycled CO_2 (green stream). The exhaust gas exit the combustor at a pressure of 300 bar (R. Allam et al., 2017; Mancuso, 2015; Rodríguez Hervás & Petrakopoulou, 2019; Scaccabarozzi et al., 2016) and are expanded in the turbine for power generation with outlet temperature and outlet pressure of approximately 720°C and 30 bar, respectively.. The exhaust gases are directed into the recuperator section for pre-heating the oxidant and the recycled CO_2 flows. According to (R. Allam et al., 2017), the recuperator is a compact multi-stream printed-circuit (Shiferaw et al., 2016) type capable of achieving pinch point temperature differences of 1-5 K (Shah & Sekulić, 2003; Smith, 2005). It is modelled as two multi-stream heat exchangers. A cold re-compressor, working with a small fraction of the exhaust gases exiting the recuperator, was added to increase the regeneration efficiency by introducing additional heat to the low-temperature heat exchanger (Zhang et al., 2020).

The flue gas is subjected to further cooling, dehumidification, and compression above critical pressure. After being compressed by the multistage compressor C-2 and cooled in cooler F-2, a small quantity of CO_2 is exported from the system in the supercritical state at 30°C. The remaining quantity is divided

https://doi.org/10.52202/077185-0144

into two flows by splitter H-2. A CO_2 fraction is mixed with oxygen from ASU to form the oxidant, while the remaining part is used for the combustor outlet temperature regulation and the turbine cooling process. The pressure of both flows is raised by pumps P-1 and P-2 before entering the recuperator.

Simulations setup and assumptions

Cycle modelling and calculations were computed in Aspen Plus (Aspen Technology, Inc, 2016). All equipment units were modelled with the blocks readily present in Aspen Plus and solved by energy and mass balance criteria. The Peng-Robinson equation of state has been used to predict the thermodynamic properties of supercritical CO_2, which allows for accurate predictions of CO_2 densities and applies to mixtures with one supercritical fluid at high pressure (Peng & Robinson, 1976; Scaccabarozzi et al., 2016). Turbines, pumps, and compressors were simulated considering the mechanical and isentropic efficiencies reported in Table 1. A base cycle thermodynamic analysis was first conducted for a combustor outlet temperature (COT) equal to 1150°C (R. Allam et al., 2017; Scaccabarozzi et al., 2016; Uysal & Uysal, 2021; Xie et al., 2023), a regenerator pinch-point set to 5°C and a hot-side temperature approach (HSTA) set to 10°C. The simulation inputs and parameters are summarised in Table 2.

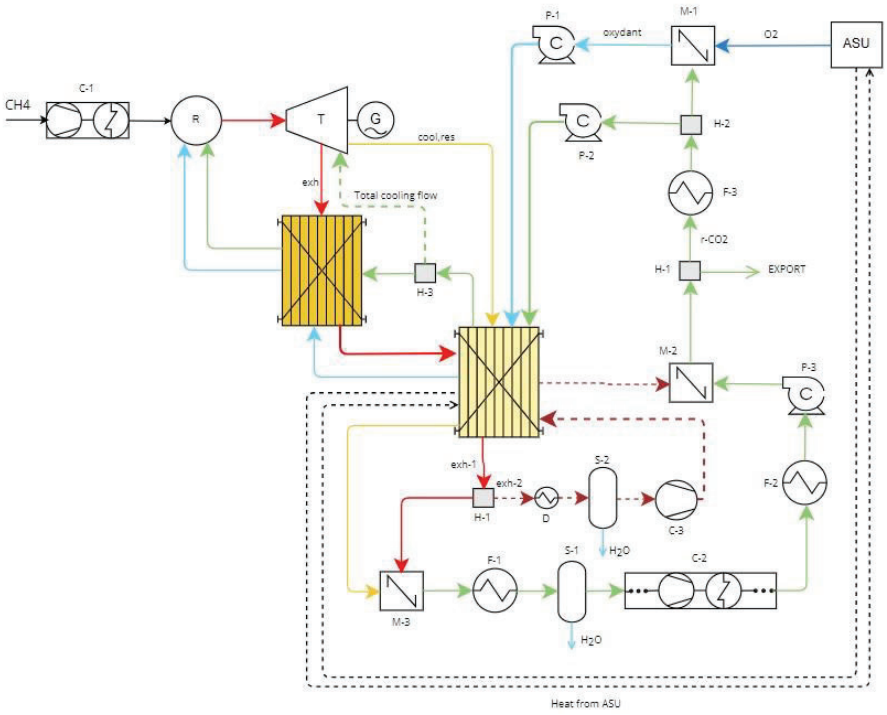

Figure 1- Flowsheet of simulation model

Table 1- Components efficiencies

Efficiency	*Value (-)*	*reference*
Turbine isentropic	0.90	(Rodríguez Hervás & Petrakopoulou, 2019)
Turbine mechanical	0.99	(Rodríguez Hervás & Petrakopoulou, 2019)
Compressor C-1, C-2, C3 polytropic	0.80	(Penkuhn & Tsatsaronis, 2016)
Compressor C-1, C-2, C3 mechanical	0.98	(Penkuhn & Tsatsaronis, 2016)
Pump P-1, P-2 polytropic	0.80	(Penkuhn & Tsatsaronis, 2016)
Pump P-1, P-2 mechanical	0.98	(Penkuhn & Tsatsaronis, 2016)
Pump P-3 efficiency	0.75	(Penkuhn & Tsatsaronis, 2016)
Pump P-3 mechanical	0.98	(Penkuhn & Tsatsaronis, 2016)

https://doi.org/10.52202/077185-0144

In addition, several constraints have been defined to perform a realistic plant simulation accurately. In particular, the COT and recuperator pinch-point target are obtained by regulating the r-CO_2 stream mass flow (recycled carbon dioxide after export) and the recuperator cold stream outlet temperature, respectively; secondary flows have been regulated by setting a constant ratio between the total cooling flow and the turbine inlet mass flow. This ratio is around 9-12% (Mancuso, 2015).

Regenerator model

This section consists of a preliminary design criteria determination of the recuperator. As (Guo, 2016) described, the recuperator cannot be modelled as a single multi-flow exchanger. In fact, the presence of significant temperature differences between the inlet and outlet on the two sides of the exchanger leads to modelling it as two multi-stream heat exchangers (MSHE): a colder temperature heat exchanger HXR1 and a hotter temperature heat exchanger HXR2 connected in series, as reported in Figure 2. The temperature of the oxidant exiting HXR2 is set so that the HSTA equals to 10°C. The temperature of the recycle exiting HXR1 is equal to the turbine cooling flow temperature, which is set to 400°C (Mancuso, 2015; Rodríguez Hervás & Petrakopoulou, 2019). The temperatures of the recycle at the hot end of HXR2 and the temperature of the oxidant at the hot end of HXR1 are adjusted to obtain a minimum temperature difference of 5°C in HXR1. In contrast, the temperature of the hot streams at the cold end of HXR1 is derived from the energy balances of the regenerator. This model and these criteria allow the recuperator to be modelled to bring it closer to a more realistic design with a better coupling of the heat exchange curves.

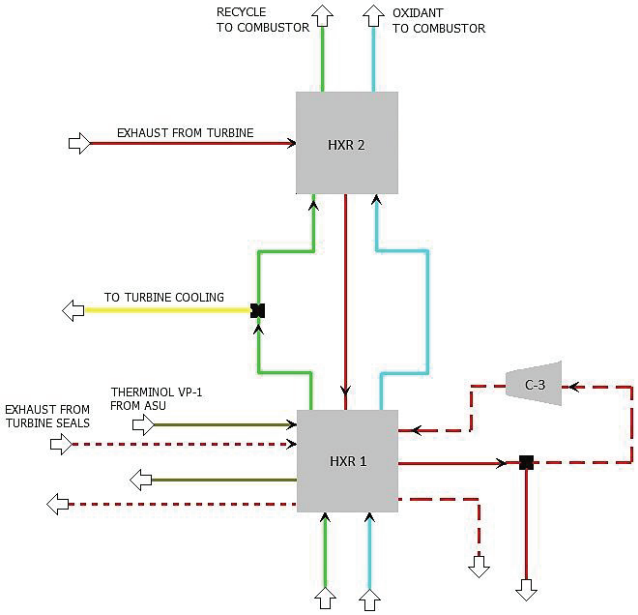

Figure 2- Flowsheet of the regenerator model

Table 2- Simulations input parameters

Parameters	**Value**	**Unit**
Combustor outlet temperature	1150	°C
Turbine inlet pressure	300	bar
Turbine outlet pressure	30	bar
Hot-side temperature approach	10	°C
$\Delta T_{PP,HXR1}$	5	°C
Minimum fluid temperature	20	°C

https://doi.org/10.52202/077185-0144

2.3 Sensitivity analysis

Further cases with different COT and HXR1 pinch-points (ΔTPP,HXR1) have been analyzed as the turbine, and the recuperator modelling significantly impact the overall system. A larger COT range has been explored to consider the maximum creep rupture strength of conventional and commercial materials, i.e. 1% CrMoV steel and novel non-conventional ones with higher maximum mechanical characteristics in high-temperature regions (R. J. Allam et al., 2013).In particular, COT has been varied between 950 °C and 1250 °C (Viswanathan et al., 2006). $\Delta T_{PP,HXR1}$ have been varied between the printed-circuited heat exchanger's lowest allowable value of 1°C and 30°C, which is used to simulate the worsening conditions of the exchanger without excessively compromising the cycle performance. The sensitivity analysis modelling setup is shown in Table 3.

Table 3- Sensitivity model setup

Target	Variables	Unit	Fixed parameters
COT	r-CO_2 total mass flow	kg/s	• Turbine and compressor efficiencies • Turbine inlet pressure (TIP) • Turbine outlet pressure (TOP) • Compressor C-2 outlet pressure • Fuel and oxygen consumption • Hot-side temperature approach (HSTA) • Cooling flows temperature • Minimum fluid temperature
$\Delta T_{PP,HXR1}$	r-CO_2 regenerator oulet temperature oxidant regenerator outlet temperature	°C	

2.4 Exergy Analysis

After a thermodynamic evaluation of the system, an exergy analysis is performed to identify the primary sources of thermodynamic losses. The exergy analysis has been computed both for the base case and for two other cases: the first with a COT similar to the reference case and $\Delta T_{PP,HXR1}$ equal to 30°C and a second case with the minimum studied COT (950°C) and a $\Delta T_{PP,HXR1}$ equal to that of the base case in order to evaluate how the various components react in terms of exergy losses to these parameters variation. Exergy can be defined as the maximum useful work obtained from a thermal system when it reaches thermodynamic equilibrium with the environment while interacting only with the environment. Exergy can be divided into four components: physical, chemical, kinetic and potential. In this work, only physical and chemical exergy are considered. The analysis is realized at the component level and the exergy of fuel ($E_{F,k}$) and product ($E_{P,k}$) as well as the exergy destruction ($E_{D,k}$) rate are defined for each k-th plant component. In fact, for a single component:

$$E_{i,k}^{tot} - E_{e,k}^{tot} - E_{D,k} = E_{F,k} - E_{P,k} - E_{D,k} = 0 \quad (1)$$

This equation demonstrates that the exergy change of a system during a process is given by the difference between the net exergy transfer through the system boundary and the exergy destroyed within the system because of irreversibility. Exergy efficiency can thus be defined for the k-th component by equation (2) and for the whole system by equation (3);

$$\varepsilon_k = \frac{E_{P,k}}{E_{F,k}} = 1 - \frac{E_{D,k}}{E_{F,k}} \quad (2)$$

$$\psi = \frac{W_{net}}{E_{fuel}} \quad (3)$$

where W_{net} is the net plant power output and E_{fuel} represents the sum of the physical and chemical exergy of pure methane.

https://doi.org/10.52202/077185-0144

Another interesting parameter to be evaluated is the k-th component exergy destruction factor, which can be calculated by equation (4):

$$\delta_k = \frac{E_{D,k}}{E_{fuel}} \quad (4)$$

It quantifies the contribution of the exergy destruction within the k-th component to the total reduction affecting the exergetic efficiency of the whole system ψ.
Exergy destruction rate and efficiency equations for the Allam plant components are summarised in Table 4.

Table 4- Exergy destruction and efficiency of the components

Component	E_D	ε
Turbine	$(E_{in}\text{-}E_{out})\text{-}W_t$	$W_t/(E_{in}\text{-}E_{out})$
Compressor/ pump	$W_{c/p}\text{-}(E_{out}\text{-}E_{in})$	$(E_{out}\text{-}E_{in})/W_{c/p}$
Combustor	$(E_{in}+E_{fuel})\text{-}E_{out}$	$E_{out}/(E_{in}+E_{fuel})$
Heat exchanger	$\sum E_{in}\text{-}\sum E_{out}$	$\sum E_{out}/\sum E_{in}$

3 RESULTS AND DISCUSSIONS

This section presents and discusses the main cycle analysis and sensitivity analysis results based on the assumptions made for the simulations that refer to various publications. Furthermore, exergy analysis results are presented to discuss the effect of the variation of key parameters on the cycle.

3.1 Base case results

In this section, the results of the thermodynamic analysis of the base case are discussed. The results shown in Table 5 demonstrate that the cycle achieves an electric efficiency of 49%, which is lower than those present in the literature, ranging between 53-56 %. Despite this difference, the efficiency obtained can be considered satisfactory as some assumptions are not favourable compared to previous studies. In fact, higher turbomachinery efficiency and a rigorous recuperator design could improve efficiencies. However, according to the regenerator heat exchange curves in Figure 3, the minimum temperature approach of 5°C is reached at the hot side of the HXR 1, and other local pinch points can be observed, demonstrating the good quality of the heat transfer. These points are obtained in correspondence to the ASU thermal carrier inlet (270°C) (Scaccabarozzi et al., 2016) and the flue gas dew point around 110°C.

3.2 Sensitivity analysis

Pinch-point sensitivity analysis

The pinch-point sensitivity analysis was performed by varying the minimum temperature difference of the HXR1 exchanger between 1°C and 30°C. This parameter, as described in section 2.3, is regulated by the temperature of the recycled CO_2 at the regenerator outlet, while that of the oxidant was kept

Table 5- Performance evaluation of the base case

Parameter	unit	results
Turbine power output	MW	449
Compressors and pumps consumption	MW	101
Net electric efficiency (LHV)	-	49%
Turbine outlet temperature	°C	727
Oxidant final temperature	°C	717
Recycle flow final temperature	°C	713
Total recycle flow rate (after export)	kg/s	967
Regenerator global UA	kW/K	36250

https://doi.org/10.52202/077185-0144

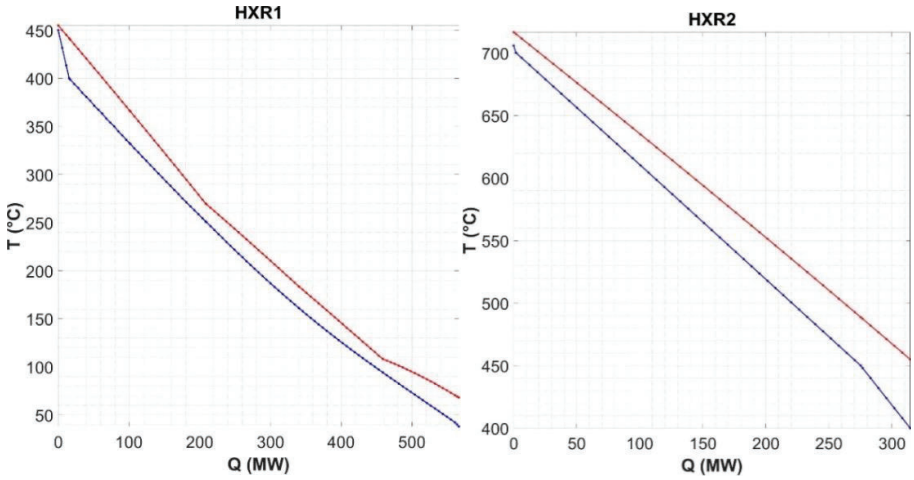

Figure 3- T-Q diagrams of the regenerator for the reference case

constant to maintain the same hot-side temperature difference of the HXR2 exchanger of 10°C. Figure 4 shows the trends of both the cycle efficiency and the temperature of the cold streams exiting the exchanger as a function of the overall UA of the regenerator. The increase of $\Delta T_{PP,HXR1}$ and, thus, the reduction of the exchanger size caused by the limited recirculation temperature reduces the cycle efficiency. This is because the cycle has to process a lower recirculation mass flow rate to maintain the energy balance in the combustor and the same COT. Furthermore, it can be deduced that it is not convenient to increase the size of the regenerator to achieve pinch-points below 5 °C because of the rapid growth of the requested area as the HSTA starts to achieve values less than 10 °C, while efficiency improvements of less than 1% are observed.

COT sensitivity analysis

The sensitivity analysis results indicate that cycle efficiency decreases for lower COT values at the same pinch-point. Although the decrease of this parameter increases the recycled flow rate, its effect is not significant enough to counterbalance the additional turbine power output at high temperatures. For a pinch-point of 5°C (reference case), efficiencies of 44%, 47%, 49% and 51% are observed for COT of 950 °C, 1050 °C, 1150°C and 1250 °C, respectively.

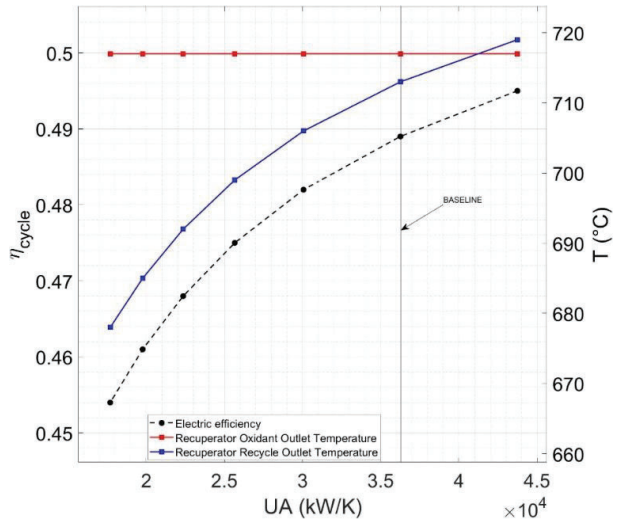

Figure 4- Base case Net electric efficiency and temperature at the outlet of the regenerator cold stream as a function of the regenerator global UA

https://doi.org/10.52202/077185-0144

A sensitivity analysis of all evaluated COTs regarding the pinch point values was also conducted. The results are displayed in Figure 5, and the efficiency trend is similar to the one presented in Figure 4. For $\Delta T_{PP,HXR1}$ values from 15 °C to 30 °C, all explored points are reported as the HSTA constraint is respected. UA lines demonstrate a relatively vertical pattern for lower temperatures, indicating a reduced COT impact on the recuperator size. A similar behaviour is observed for $\Delta T_{pp,HXR1}$ = 10 °C. For $\Delta T_{pp,HXR1}$ temperatures below 10 °C, the recuperator size changes slightly from 1050 °C to 1150 °C while for COT of 950 °C, the UA value tends to increase considerably. This effect is due to the significant increase of the recycled CO_2 flow rate at lower turbine inlet temperature and lower pinch-point approcach For COT = 1250 °C, the regenerator UA tends to be greater for $\Delta T_{PP,HXR1}$ values from 15 °C to 30 °C while for $\Delta T_{pp,HXR1}$ temperatures below 10 °C the regenerator UA is not defined for the HSTA constraint. This effect is due to the presence of local pinch points, i.e., in correspondence with the flue gas dew point (around 110°C), which requires more exchanger area to be satisfied. A more straightforward representation of the efficiency variation as a function of the size of the recuperator is presented in Figure 6.

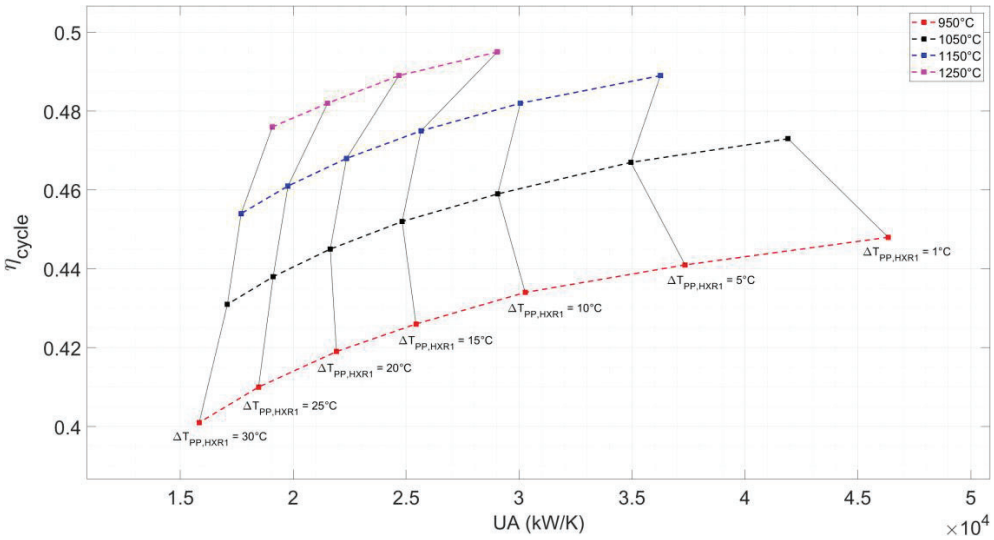

Figure 5- Net electric efficiency vs. global recuperator UA as a function of HXR1 minimum temperature difference

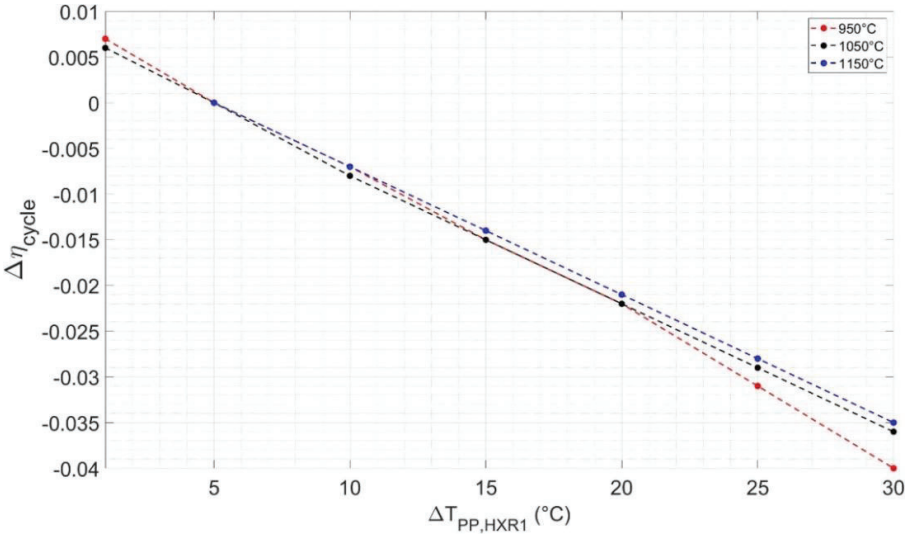

Figure 6- Electric efficiency variation as a function of HXR1 minimum temperature difference

https://doi.org/10.52202/077185-0144

The finding is crucial as it demonstrates the possibility of reducing the size of the recuperator (thus its cost) in correspondence with values of $\Delta T_{pp,HXR1}$ up to 10°C without a significant efficiency penalty. In fact, up to 10°C, a reduction of the efficiency of less than one percentage point is observed regardless of the COT. For $\Delta T_{pp,HXR1}$ larger than 10°C, due to the significant recycled CO_2 mass flow rate, reducing the recuperator size is less convenient at 950°C compared to the cases with higher COT.

3.3 Exergy analysis

The results of the exergetic analysis at the component level for the three studied cases are shown in Table 6. Case 1 refers to COT=1150°C and $\Delta T_{pp,HXR1}$ = 30°C and case 2 refers to COT=950°C and $\Delta T_{pp,HXR1}$ = 5°C. As shown in Table 6, most of the exergy destruction occurs in the combustor with more than one-quarter of the total fuel supply exergy for all cases. Despite relatively high efficiency, the recuperator and turbine are ranked second and third for the base case and case 1, while the opposite happens for case 2. The multistage compressor C-2 presents the fourth-highest exergy destruction with a decreasing exergy destruction factor when regenerator dimensions are reduced. The compression/pumping and condensation groups follow the pattern with the lowest exergy destructions. The total exergy destruction of the base case was found to be 303 MW. Moreover, referring to that value, the lower the recuperator dimensions or the lower the COT, the higher the total plant exergy destruction. The total plant losses for case 1 and case 2 are greater than those of the base case of 23 MW and 33 MW, respectively. In Figure 7, apart from the combustor, which has the highest losses, the losses of the other components that contribute the most to cycle inefficiencies are represented in a bar graph. In fact, a reduction of the regenerator size (case 1) not only generates an increase in losses to the regenerator but also leads to an improvement, although slight, in the exergy performance of the C-2 multistage compressor thanks to the decrease of the total recycled flow rate in the cycle. On the other hand, a decrease in the COT presents a slight worsening of the turbine and C-2 compressor performance, while those of the other components remain almost unchanged.

Table 6- Results of exergy analysis.

Simulation	Base case			Case 1			Case 2		
	E_D	ε	δ	E_D	ε	δ	E_D	ε	δ
Component	MW	%	%	MW	%	%	MW	%	%
R	160.63	86.6%	27.68	161.91	85.9%	27.90	183.39	84.0%	31.60
T	38.40	92.1%	6.62	36.42	92.1%	6.28	40.56	91.5%	6.99
C-1	0.85	72.2%	0.15	0.85	72.2%	0.15	0.85	72.2%	0.15
C-2	14.39	70.9%	2.48	13.53	70.9%	2.33	16.63	70.9%	2.87
C-3	2.00	83.4%	0.34	2.10	83.8%	0.36	1.89	83.6%	0.33
HXR1	42.72	93.7%	7.36	56.48	91.4%	9.73	41.65	94.5%	7.18
HXR2	8.48	99.2%	1.46	10.51	98.9%	1.81	8.22	99.2%	1.42
P-1	2.20	71.5%	0.38	2.18	71.7%	0.38	2.21	71.4%	0.38
P-2	4.04	79.7%	0.70	3.67	80.1%	0.63	4.84	79.6%	0.83
P-3	3.56	58.3%	0.61	3.35	58.3%	0.58	4.12	58.3%	0.71
B5	4.76	97.0%	0.82	7.38	95.3%	1.27	3.89	97.9%	0.67
F-1	1.62	99.2%	0.28	1.63	99.1%	0.28	1.53	99.3%	0.26
F-2	2.57	98.7%	0.44	2.29	98.8%	0.40	2.90	98.8%	0.50
TOTAL	303	49.3%	-	326	46%	-	336	44.7%	-

https://doi.org/10.52202/077185-0144

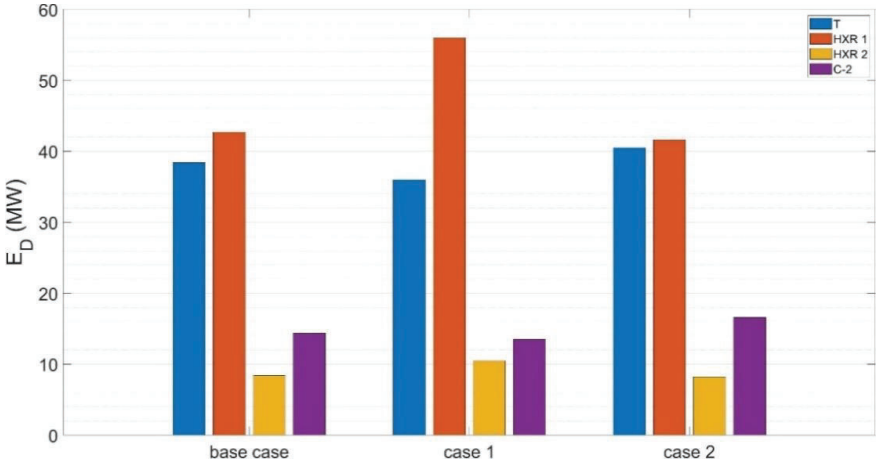

Figure 7- Exergy destruction in key components

4 CONCLUSIONS

In this work, an Allam cycle model was presented and studied firstly through a generical analysis of its thermodynamic performances and then at the component level from an exergetic perspective. The results have shown that the plant can reach a net electric efficiency of up to 51% and an exergetic efficiency of 51.5%, which may be higher than those obtained with other CO_2 capture technologies. The difference of -5 percentage point with respect to the value calculated in (Scaccabarozzi et al., 2016) appears to be due to the more conservative assumptions on the regenerator pinch point with a fixed cooling flow temperature on the turbomachinery efficiencies and to the turbine cooling system modelling which not considered an accurate expansion model, i.e. the El-Masri's continuous expansion model developed in (Scaccabarozzi et al., 2016). It has been demonstrated that reducing the size of the recuperator from 45000 kW/K to 30000 kW/K may represent a good trade-off between the heat exchanger dimension and the related cycle performance, causing an efficiency reduction of less than -1 percentage point. Finally, an exergy evaluation has provided that CO_2 compression and pumping are the components with the most potential for improvement because of their low exergy efficiency.

NOMENCLATURE

Abbreviations

ASU	air separation unit
COT	combustor outlet temperature
HTSA	hot-side temperature approach
LHV	low heating value
MSHE	multi-streams heat exchanger
r-CO_2	recycled carbon dioxide
res	residual
SCOC-CC	semi-closed oxy-combustion combined cycle

Symbols

ε	component exergy efficiency	
ψ	global exergy efficiency	
δ	exergy destruction factor	
ΔT_{pp}	pinch-point temperature difference	(°C)
$\dot{E}$	exergy flow balance	(MW)
T	temperature	(°C)
$\dot{m}$	mass flow rate	(kg/s)

https://doi.org/10.52202/077185-0144

W_{net}	net electric power	(MW)

Subscript

c	compressor
D	destroyed
exh	exhaust
F	fuel
in	inlet
int	turbine inlet
k	component k
out	outlet
p	pump
P	product
t	turbine
tot	total

REFERENCES

Allam, R. J., Palmer, M. R., Brown, G. W., Fetvedt, J., Freed, D., Nomoto, H., Itoh, M., Okita, N., & Jones, C. (2013). High efficiency and low cost of electricity generation from fossil fuels while eliminating atmospheric emissions, including carbon dioxide. *Energy Procedia*, *37*(February 2014), 1135–1149. https://doi.org/10.1016/j.egypro.2013.05.211

Allam, R., Martin, S., Forrest, B., Fetvedt, J., Lu, X., Freed, D., Brown, G. W., Sasaki, T., Itoh, M., & Manning, J. (2017). Demonstration of the Allam Cycle: An Update on the Development Status of a High Efficiency Supercritical Carbon Dioxide Power Process Employing Full Carbon Capture. *Energy Procedia*, *114*(November 2016), 5948–5966. https://doi.org/10.1016/j.egypro.2017.03.1731

Aspen Technology, Inc. (2016). http://www.aspentech.com/

Bolland, O., & Mathieu, P. (1998). Comparison of two CO2 removal options in combined cycle power plants. *Energy Conversion and Management*, *39*(16–18), 1653–1663. https://doi.org/10.1016/s0196-8904(98)00078-8

Chowdhury, A. S. M. A., Bugarin, L., Badhan, A., Choudhuri, A., & Love, N. (2016). Thermodynamic analysis of a directly heated oxyfuel supercritical power system. *Applied Energy*, *179*, 261–271. https://doi.org/10.1016/j.apenergy.2016.06.148

Figueroa, J. D., Fout, T., Plasynski, S., McIlvried, H., & Srivastava, R. D. (2008). Advances in CO2 capture technology-The U.S. Department of Energy's Carbon Sequestration Program. *International Journal of Greenhouse Gas Control*, *2*(1), 9–20. https://doi.org/10.1016/S1750-5836(07)00094-1

Guo, J. (2016). Design analysis of supercritical carbon dioxide recuperator. *Applied Energy*, *164*, 21–27. https://doi.org/10.1016/j.apenergy.2015.11.049

Iantovski, E., & Mathieu, P. (1997). Highly efficient zero emission CO2-based power plant. *Energy Conversion and Management*, *38*(SUPPL. 1). https://doi.org/10.1016/s0196-8904(96)00260-9

IPCC Panel. (2014). *Climate Change 2014: Synthesis Report*. 1–151.

Jericha, H., Sanz, W., & Göttlich, E. (2008). Design concept for large output Graz Cycle gas turbines. *Journal of Engineering for Gas Turbines and Power*, *130*(1), 1–14. https://doi.org/10.1115/1.2747260

Mancuso, L. (2015). Oxy-Combustion Turbine Power Plants. *Ieaghg*, *August*, 636. https://ieaghg.org/docs/General_Docs/Reports/2015-05.pdf

Peng, D. Y., & Robinson, D. B. (1976). A New Two-Constant Equation of State. *Industrial*

https://doi.org/10.52202/077185-0144

and Engineering Chemistry Fundamentals, *15*(1), 59–64. https://doi.org/10.1021/i160057a011

Penkuhn, M., & Tsatsaronis, G. (2016). Exergy Analysis of the Allam Cycle. *The 5th International Symposium - Supercritical CO2 Power Cycles*, 1–18. http://sco2symposium.com/papers2016/OxyFuel/040paper.pdf

Rodríguez Hervás, G., & Petrakopoulou, F. (2019). Exergoeconomic Analysis of the Allam Cycle. *Energy and Fuels*, *33*(8), 7561–7568. https://doi.org/10.1021/acs.energyfuels.9b01348

Rubin, E. S., Mantripragada, H., Marks, A., Versteeg, P., & Kitchin, J. (2012). The outlook for improved carbon capture technology. *Progress in Energy and Combustion Science*, *38*(5), 630–671. https://doi.org/10.1016/j.pecs.2012.03.003

Scaccabarozzi, R., Gatti, M., & Martelli, E. (2016). Thermodynamic analysis and numerical optimization of the NET Power oxy-combustion cycle. *Applied Energy*, *178*, 505–526. https://doi.org/10.1016/j.apenergy.2016.06.060

Shah, R. K., & Sekulić, D. P. (2003). Selection of Heat Exchangers and Their Components. In *Fundamentals of Heat Exchanger Design*. https://doi.org/10.1002/9780470172605.ch10

Shiferaw, D., Carrero, J. M., & Le Pierres, R. (2016). Economic analysis of SCO2 cycles with PCHE recuperator design optimisation. *The 5th International Symposium - Supercritical CO2 Power Cycles*, 1–13.

Smith, R. (2005). Chemical Process Design and Integration. In *John Wiley & Sons, Ltd*.

Uysal, D., & Uysal, B. Z. (2021). Thermodynamic analysis of the Allam cycle and its pressure sensitivity. *Journal of Thermal Engineering*, *7*(6), 1448–1456. https://doi.org/10.18186/thermal.990813

Viswanathan, R., Sarver, J., & Tanzosh, J. M. (2006). Boiler materials for ultra-supercritical coal power plants - Steamside oxidation. *Journal of Materials Engineering and Performance*, *15*(3), 255–274. https://doi.org/10.1361/105994906X108756

Wall, T. F. (2007). Combustion processes for carbon capture. *Proceedings of the Combustion Institute*, *31 I*(1), 31–47. https://doi.org/10.1016/j.proci.2006.08.123

Xie, M., Chen, L., Wu, K., Liu, Z., Lin, J., Jiang, C., Xie, S., & Zhao, Y. (2023). A novel peak shaving approach to improving load flexibility of the Allam cycle by integrating cold energy storage. *Journal of Cleaner Production*, *386*(October 2022), 135769. https://doi.org/10.1016/j.jclepro.2022.135769

Zhang, X., Yu, L., Li, M., & Song, P. (2020). Simulation of a Supercritical CO2 Recompression Cycle with Zero Emissions. *Journal of Energy Engineering*, *146*(6), 1–18. https://doi.org/10.1061/(asce)ey.1943-7897.0000711

ACKNOWLEDGEMENT

This research has received a financial contribution from the National Recovery and Resilience Plan (PNRR), Mission 4 Component 2 Investment 1.3 - Call for tender No. 1561 of 11.10.2022 of Ministero dell'Università e della Ricerca (MUR); funded by the European Union – NextGenerationEU.

Dr. Guido Francesco Frate acknowledges the financial contribution received by the Ministry of University and Research (MUR) as part of the FSE REACT-EU - PON 2014-2020 "Research and Innovation" resources – Green/Innovation Action - DM MUR 1062/2021 - Title of the Research: *Soluzione e tecnologie innovative per la generazione di potenza e le macchine a fluido nella transizione verde*.

Dr. Gnandjuet Gaston Brice Dago acknowledges the financial Italian Operative National Plan (Piano Operativo Nazionale, PON) in the framework of the project Ricerca e Innovazione 2014−2020 (PON R&I) – Azioni IV.4 e IV.5 “Dottorati di ricerca su tematiche dell'innovazione e green” (DM MUR 1061/2022) e IV.6 “Contratti di ricerca su tematiche dell'innovazione e green” (DM MUR 1062/2022).

https://doi.org/10.52202/077185-0144